Cytosine in Context: A Theoretical Study of Substituent Effects on the Excitation Energies of 2-Pyrimidinone Derivatives

Kurt A. Kistler and Spiridoula Matsika*

Department of Chemistry, Temple University, Philadelphia, Pennsylvania 19122

Received: June 6, 2007

The ultrafast radiationless decay mechanism for cytosine has been shown to be in part dependent upon high vertical excitation, while slower fluorescence displayed in some cytosine analogs is generally linked to lower vertical excitation energies. To probe how excitation energies relate to pyrimidine structure, substituent effects on the vertical excitation energies for a number of derivatives of 2-pyrimidin-(1*H*)-one (2P) have been calculated using multireference configuration-interaction ab initio methods. Substitutions using groups with π electron donating, withdrawing and conjugation-extending properties at the C^4 and C^5 positions on the 2P system give predictive trends for the first three singlet excited-state energies. The S_1 $\pi\pi^*$ energies of 2P derivatives involving C^4 substitution vary linearly with the Hammett substituent parameter σ_P^+. Cytosine is shown to have the highest bright $\pi\pi^*$ energy of the 2P derivatives presented, with that energy being strongly dependent on the position, orientation, and geometry of the C^4-amino. A simple description of the predictive energetic trends for the bright $\pi\pi^*$ energies using frontier molecular orbital theory is presented, based on the character of the HOMO and LUMO orbitals for each derivative. The results of this study expand the current understanding of the photophysical behavior of the DNA pyrimidine bases and could be useful in the design of analogs where particular spectral properties are desired.

1. Introduction

The ability of photoexcited cytosine (Cyt, Figure 1) to undergo ultrafast radiationless decay on the order of 1 ps or less[1−4] has been shown to depend on the topological features of the bright S_1 adiabatic potential energy surface (PES).[5−12] These features, when combined, can facilitate radiationless deactivation to the ground state, enabled by conical intersection seams, regions where the probability of nonadiabatic transitions to S_0 is high.[13−15] Figure 2 shows the S_1 PES for cytosine along two directions that lead to radiationless decay through conical intersections, based on our previous multireference configuration-interaction (MRCI) results.[12,16] Vertical excitation is ca. 0.8 eV above the minimum energy stationary point on the S_1 PES (experimental value is about 0.7 eV[17,18]), and ca. 1.1 eV above the lowest energy S_0/S_1 conical intersection seam point, creating a vibrationally excited population with strong momentum away from the Franck−Condon region. The lack of significant barriers on the S_1 PES in directions toward the lowest S_0/S_1 conical intersection seam points, combined with energetic accessibility of these seam points relative to minima on the S_1 surface, further serve to facilitate radiationless decay in terms of the topology of the bright excited PES.[12] This is contrasted with the Cyt analog 5-methyl-2-pyrimidin-(1*H*)-one (5M2P),[16,19,20] which has the same heterocyclic 2-pyrimidin-(1*H*)-one (2P) ring and carbonyl system, but has a methyl group at C^5, while cytosine has an amino group at C^4. Aqueous solution of this analog fluoresces after UV excitation with a lifetime thousands of times longer than that of cytosine.[21] 5M2P is known experimentally,[19] and was calculated theoretically,[16] to have lower excitation energy than cytosine. Figure 2 shows the S_1 PES for 5M2P along the same two directions as in cytosine, based on our previous MRCI results.[16] The minima on the two S_0/S_1 seams are only slightly lower than vertical excitation on S_1, and the global S_1 minimum is about 0.3 eV lower than the lowest energy point on the seam. Therefore, a trapping bowl S_1 topology is observed where vibrational states can be bound, thus greatly increasing the fluorescence lifetime of 5M2P compared to that of cytosine. These differences in the S_1 PESs of these two bases are interesting since the two bases were shown to distort almost identically for virtually all excited-state stationary points and conical intersections. Thus, it seems that energetic differences between the bases, rather than conformational differences, could be the dominant reason for the different photophysical behavior of these bases. The largest energetic difference seen on the bright

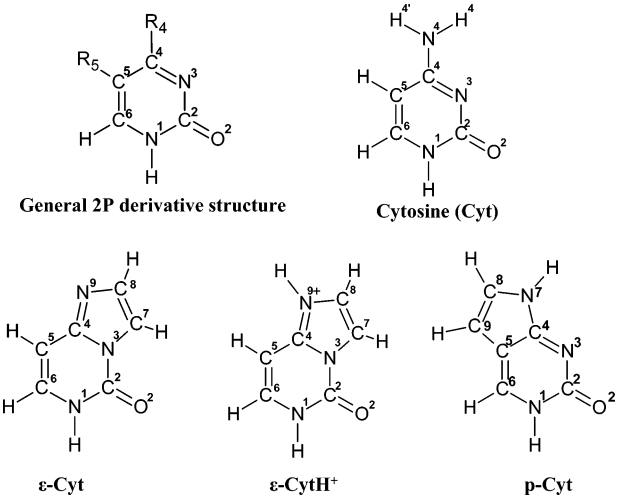

Figure 1. Structures of the general 2P derivative, Cyt, ϵ-Cyt, ϵ-CytH^+, and p-Cyt, with numbering of atoms used in this paper. Specific 2P derivatives are itemized by R_4 and R_5 groups in Table 1.

* To whom correspondence should be addressed. E-mail: smatsika@temple.edu.

10.1021/jp074361d CCC: $37.00
Published on Web 08/16/2007

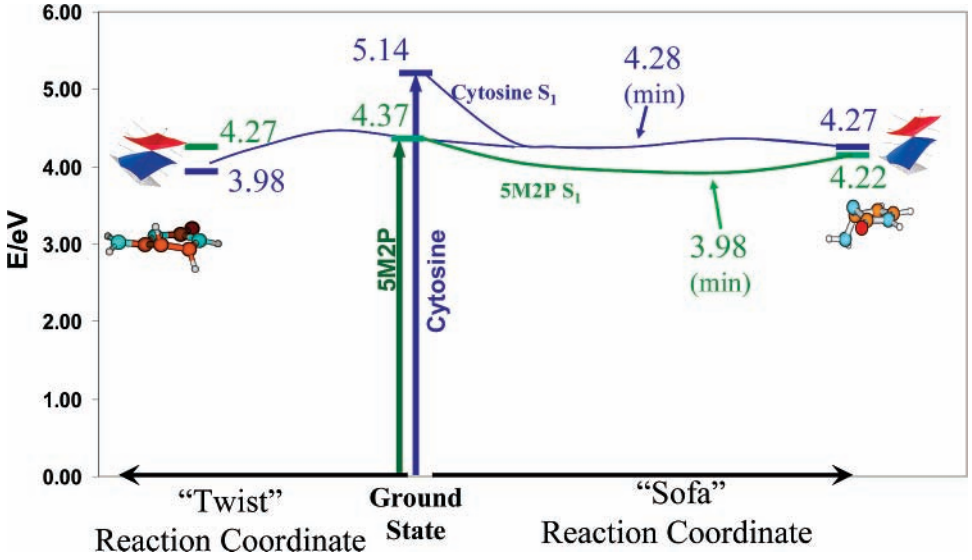

Figure 2. Photophysically important regions of the S_1 surfaces of Cyt and 5M2P are shown for comparison. Energies of vertical excitations, conical intersections, and the S_1 minimum for 5M2P are in eV, referenced to the ground-state minimum for each base. Blue and green lines represent S_1 $\pi\pi^*$ minimum energy paths calculated using MRCI, for Cyt and 5M2P, respectively. Data are taken from ref 12.

excited states of these two bases is at vertical excitation, with Cyt being higher than 5M2P by about 0.7 eV, as measured experimentally in aqueous solution,[19,21,22] and calculated in our work. A similar difference in excitation energies is seen between adenine, which decays radiationless, and the fluorescent adenine analog, 2-aminopurine, which differs from adenine only in the position of an amino group, but has an excitation energy about 0.5 eV lower than adenine, as measured experimentally.[23−26] Adenine[27−31] and 2-aminopurine[31−33] have also been studied theoretically. As the excitation difference in Cyt seems to be directly related to its radiationless decay, it is important to understand the reason for the initial excitation difference between Cyt and 5M2P. While there have been many theoretical studies on the absorption energies and general photophysical behavior of Cyt,[5−12,34−37] as well as other DNA bases[27−30,33,37−44] and DNA base analogs,[16,26,31−33,45,46] the relationship between structure and absorption spectra of the bases and their analogs has, to our knowledge, not been specifically addressed.

To probe this relationship, a series of 2P derivatives were studied theoretically by varying functional groups at ring positions C^4 and C^5, and calculating vertical excitation energies for the optimized ground-state geometries using methods described in Section 2. The results of this study show that, when compared to known experimental absorbance data, these substituent effects display predictive trends not only of the absorbance maxima but also the energy gap between S_1 and S_2. As such, these energetic trends could be useful for researchers, such as those interested in the design of pyrimidine analogs where particular spectral properties are desired. A similar substitution treatment has been used for decades in the field of dye coloration,[47,48] such as with azomethine dyes,[49,50] and recently it has also been used to tune the spectral properties of organic light-emitting diode compounds, such as pyrazoline derivatives,[51] and also poly(*p*-phenylenevinylene) oligomers.[52]

Figure 1 shows the general 2P derivative structure with ring numbering used in this study. Table 1 lists the derivatives presented by number and the R_4 and R_5 groups for each, with 2P itself as **1**. 2P derivatives with R_5 = H and substitution at C^4 are as follows: Cyt (**2**), 4-nitroso-2-pyrimidin-(1*H*)-one (**3**), 4-cyano-2-pyrimidin-(1*H*)-one (**4**), 4-formyl-2-pyrimidin-(1*H*)-one (**5**), 2-oxo-1,2-dihydropyrimidine-4-carbonyl fluoride (**6**), 4-carboxymethyl-2-pyrimidin-(1*H*)-one (**7**), 4-carboxyl-2-pyrimidin-(1*H*)-one (**8**), 4-ethenyl-2-pyrimidin-(1*H*)-one (**9**), 4-hydroxyl-2-pyrimidin-(1*H*)-one (**10**, tautomer of uracil), N^4-acetylcytosine (**11**), 4-fluoro-2-pyrimidin-(1*H*)-one (**12**), and N^4-vinylcytosine (**13**). Derivatives of 2P with R_4 = H and C^5 substitution are as follows: 5-methyl-2-pyrimidin-(1*H*)-one (**14**), 5-fluoro-2-pyrimidin-(1*H*)-one (**15**), 5-amino-2-pyrimidin-(1*H*)-one (**16**), 5-nitroso-2-pyrimidin-(1*H*)-one (**17**), 5-vinyl-2-pyrimidin-(1*H*)-one (**18**), 5-formyl-2-pyrimidin-(1*H*)-one (**19**), 5-(2-aminoenthenyl)-2-pyrimidin-(1*H*)-one (**20**), 5-carboxyl-2-pyrimidin-(1*H*)-one (**21**), 5-cyano-2-pyrimidin-(1*H*)-one (**22**), and 5-nitro-2-pyrimidin-(1*H*)-one (**23**). Pyrrolocytosine (p-Cyt, Figure 1) is included since its second fused ring attaches at C^4 and C^5, and it includes an amine nitrogen at C^4. N3,N^4-ethenocytosine (ϵ-Cyt) and its N^9-H conjugate acid (ϵ-CytH$^+$) are also included in this study (Figure 1).

2. Methods

The geometries for all species presented in this report are ground state (GS) minima optimized at the MP2/6-31G(d,p) level using the Gaussian03 suite of programs[53] with C_S symmetry constraints, unless specified otherwise. Excitation energies were obtained using MRCI, as described below. Molecular orbitals (MO) were obtained from a state-averaged multiconfiguration self-consistent field (SA-MCSCF) procedure averaged over the first four singlet states (S_0 to S_3), using Dunning's cc-pvdz atomic orbital basis sets.[54] The complete active set of orbitals (CAS) included one nitrogen lone pair (LP), designated as n_N, one oxygen LP, designated as n_O, and all π orbitals, or as many π orbitals as could be managed in the calculation (maximum of 10 π), while maintaining core 1s, σ, and additional n (LP) orbitals as doubly occupied. For example, 2P was assigned a CAS of 1 n_N, 1 n_O, and all 7 π orbitals occupied in total by 12 electrons. This arrangement is denoted as (12,9), where (*l*,*m*) denotes *l* electrons in *m* active orbitals. From 2520 to about 70 000 reference configurations were generated from the SA-MCSCF calculation, depending on CAS size. These references were then used for MRCI, where all core 1s and σ orbitals were maintained as frozen, and single excitations were allowed from the CAS orbitals to the virtual orbitals. This generated up to about 25 million configurations in the MRCI expansion, depending on CAS size. Increasing

TABLE 1: C^4 and C^5 Derivatives of 2P and Bicyclic Cyt Analogs[a]

C^4 Derivatives (R_5 = H)

label	R_4	type	symm, CAS	S_1, $\pi\pi^*$	S_2, $n_N\pi^*$	S_3, $n_O\pi^*$	expt[g]
1	H		C_S, (12,9)	4.49	4.55	5.14	4.04[71]
2	NH_2	X	C_1, (14,10)	4.91	5.30	5.66	4.67[72]
2′	NH_2	X	C_S, (14,10)	4.95	5.43	5.78	
2″	NH_2[b]	X	C_1 (12,9)	4.55	4.65	5.10	
3	NO	Z	C_S, (16,11)	3.95	4.22	4.73	
3′	NO[c]	Z	C_S, (16,11)	4.04	4.24	4.75	
4	CN	Z	C_S, (18,12)	4.11	4.30	4.78	3.61[73]
5	CHO	Z	C_S, (16,11)	4.12	4.33	4.84	
6	CFO	Z	C_S, (18,12)	4.05	4.23	4.72	
7	CO_2CH_3	Z	C_S, (18,12)	4.16	4.27	4.80	3.73[73]
8	CO_2H	Z	C_S, (18,12)	4.14	4.27	4.79	3.76[73]
9	$CH{=}CH_2$	C	C_S, (16,11)	4.32	4.41	4.94	
10	OH	X	C_S, (14,10)	4.93	5.45	5.83	
10′	OH[d]	X	C_S, (14,10)	4.85	5.20	5.56	
10″	OH[e]	X	C_1, (12,9)	4.72	4.99	5.37	
11	$NHCOCH_3$	X	C_S, (18,12)	4.63	5.13	5.51	4.11[74]
12	F	X	C_S, (14,10)	4.84	5.26	5.61	
13	$NHCH{=}CH_2$	X	C_S, (18,12)	4.84	5.30	5.63	

C^5 Derivatives (R_4 = H)

label	R_5	type	symm, CAS	S_1, $\pi\pi^*$	S_2, $n_N\pi^*$	S_3, $n_O\pi^*$
14	CH_3		C_1, (12,9)	4.46	4.53	5.11
15	F	X	C_S, (14,10)	4.36	4.48	4.98
16	NH_2	X	C_1, (12,9)	4.30	4.49	5.02
16′	NH_2	X	C_S, (12,9)	4.15	4.49	4.99
16″	NH_2[f]	X	C_1, (12,9)	4.47[f]	4.48[f]	5.07
17	NO	Z	C_S, (16,11)	4.24	4.55	5.15
18	$CH{=}CH_2$	C	C_S, (16,11)	4.31	4.58	5.17
19	CHO	Z	C_S, (16,11)	4.33	4.58	5.18
20	$CH{=}CHNH_2$	X	C_S, (18,12)	4.05	4.58	5.15
21	CO_2H	Z	C_S, (18,12)	4.49	4.61	5.21
22	CN	Z	C_S, (18,12)	4.44	4.56	5.14
23	NO_2	Z	C_S, (18,12)	4.47	4.56	5.12

Bicyclic Cyt Analogs

label	symm, CAS	S_1	S_2	S_3	expt
ϵ-$CytH^+$	C_S, (14,10)	5.00 ($\pi\pi^*$)	6.31 (n_O^*)	6.39 ($n_O\pi^*$)	4.31[69]
ϵ-Cyt	C_S, (18,12)	5.40 ($\pi\pi^*$)	6.21 ($n_N\pi^*$)	6.57 ($\pi\pi^*$)	4.61[69]
p-Cyt	C_S, (18,12)	3.99 ($\pi\pi^*$)	4.97 ($n_N\pi^*$)	5.39 ($n_O\pi^*$)	3.59[70]

[a] Listed for each derivative are the labels used for discussion in the text, substituent at C^4 or C^5, substituent type in terms of π interaction with the ring, symmetry, CAS used in the MRCI calculation, the first three excited-state energies, in eV, calculated at the MRCI level, and experimental energies for S_1. [b] **2″**: Cyt C_1 with amino rotated 90° out of ring plane. [c] **3′**: C_S geometry with nitroso O pointing away from N^3. [d] **10′**: C_S geometry with the hydroxyl H pointing away from N^3. [e] **10″**: OH rotated 90° out of ring plane. [f] **16″**: C_1 ground state with amino rotated 90° out of ring plane. For **16″** $S_1 = n_N\pi^*$ and $S_2 = \pi\pi^*$. [g] Based on λ_{max} of pH 7 aqueous solutions, except for **8**, which is based on λ_{max} of pH 1 aqueous solution.

dynamical correlation by including configurations involving double excitations or excitations from the σ orbitals was not done since this was prohibitively expensive for the larger derivatives. This study, however, focuses on qualitative energetic trends within the same level of theory for a collection of similar molecules and the approach used here proved to be successful in reproducing the experimentally observed trends. The error on the predicted excitation energies is ca. 0.4 eV as has been seen in previous work and is reaffirmed here.

It should be noted that the CAS for some C_1 geometries where the C^4 or C^5 substituent was rotated out of the ring plane, such as 4-amino rotamers of **2**, the 4-hydroxyl rotamer **10″**, and **16** was (12,9) since a preferred (14,10) CAS, which would include the amino or hydroxyl LP, could not be obtained. The influence of the CAS size on the MRCI S_1 $\pi\pi^*$ energy has been estimated by using a (14,10) CAS for **16′**; S_1 is 4.00 eV, compared to 4.15 eV with a (12,9) CAS. The $n\pi^*$ states for these two different active spaces are not significantly different. SA-MCSCF and MRCI calculations were carried out using the COLUMBUS Quantum Chemistry Program Suite.[55−57] Molecular visualization and graphical rendering was done with MOLDEN.[58]

3. Results and Discussion

The first three singlet excited-state energies, symmetry, and CAS for all species in this study are presented in Table 1. For all C^4 and C^5 2P derivatives the bright excited state is S_1 $\pi\pi^*$, corresponding primarily to excitation from the HOMO π to the LUMO π^*, S_2 is $n_N\pi^*$ from excitation of the N^3 LP, and S_3 is $n_O\pi^*$ from excitation of the O^2 LP (see Figure 1 for atom numbering). The reference system is 2P (**1**). Results specific to Cyt are presented in section 3.1, C^4 derivatives are presented in section 3.2, and C^5 derivatives are presented in section 3.3. The Cyt analogs p-Cyt, ϵ-Cyt, and ϵ-$CytH^+$ are presented in section 3.4.

3.1. Cytosine. The S_1 energy for 2P is 4.49 eV, with S_2 being almost degenerate with S_1 at 4.55 eV and S_3 at 5.14 eV. Substituting at C^4 with an amino group gives Cyt (Figure 1), where the symmetry of the GS minimum is C_1 (**2**). The amino

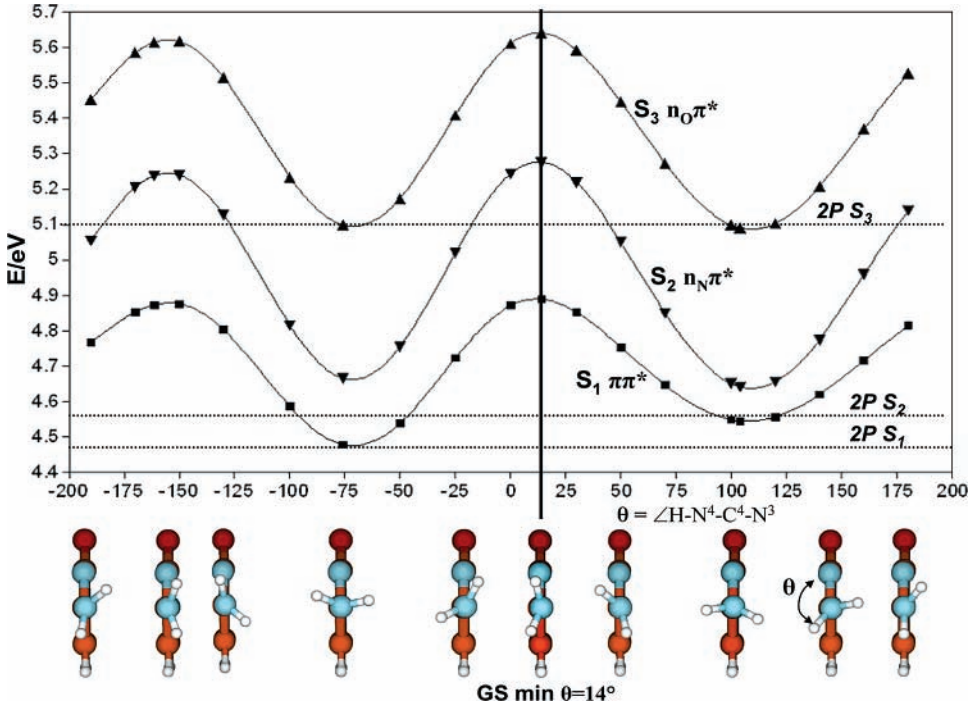

Figure 3. Excited-state energies as a function of amino rotation in Cyt. The first three excited-state energies (MRCI(12,9)) are shown. θ is the dihedral angle formed from the tetrad of atoms N^3, C^4, N^4, and the amino hydrogen closest to N^3 in the ground-state minimum geometry ($\theta = 14°$ for GS Cyt). For all geometries shown $S_1 = \pi\pi^*$, $S_2 = n_N\pi^*$, and $S_3 = n_O\pi^*$.

is pyramidalized and slightly tilted away from N^3. For **2**, S_1 is 4.91 eV, S_2 is 5.30 eV, and S_3 is 5.66 eV. The amino group increases vertical excitation by 0.4 eV, and also increases the S_1/S_2 energy gap by about 0.4 eV, compared to **1**. Constraining the symmetry of Cyt to C_S (**2′**) increases S_1 to 4.95 eV and increases the S_1/S_2 energy gap to about 0.5 eV. These results imply that the higher vertical excitation energy of Cyt, as well as the lifting of degeneracy of S_2 with S_1, is a direct result of π overlap of the N^4 π LP with the ring, which is enhanced when the system is planar. Indeed, the C^4-N^4 bond length in **2** is 1.37 Å, 0.11 Å shorter than the average C−N single bond,[59] showing partial double-bond character of this bond, and this bond in **2′** is shorter still at 1.36 Å, showing more double-bond character.

The influence of the orientation of the amino group on the excitation energies of Cyt is shown in Figure 3, where starting from the C_1 GS geometry the amino group is rotated about the C^4-N^4 bond. The first three excited-state energies are plotted as a function of $\theta = \angle N^3-C^4-N^4-H^4$ dihedral angle. Rotamers with maximum excitation energies are close to GS geometry ($\theta = 14°$) and to geometries where the amino is rotated about 180° compared to GS ($\theta = -161.5°$), both orientations commensurate with maximum π overlap with the ring. Likewise, rotamers with minimum energies correspond to the amino N−H bond being approximately perpendicular to the ring plane ($\theta = -76°$ and 100°), where π overlap is minimal. The S_1-S_2 gap also depends on amino orientation, being large where S_1 is a maximum and small where S_1 is a minimum. The monotonic sinusoidal character of the energy curves implies that the influence is from the N^4 π LP only, and not from the amino hydrogens interacting with the N^3 LP. The dotted horizontal lines in the plot correspond to the vertical excitation energies of 2P. It is clear that simply rotating the amino group to be perpendicular to the ring generates excited-state energies almost as though the amino group was absent entirely. The main normal mode of C_1 Cyt corresponding to this amino group rotation is calculated to be about 360 cm^{-1} for the ground state at the MP2 level. This implies that amino rotation in the isolated free base is somewhat labile, and absorption energies could be influenced by this motion.

3.2. C^4 Substituents. To probe the electronic influence at C^4 in a more general sense, vertical excitation energies were calculated for 2P derivatives, which all have the main 2P ring system along with a side group R_4 (Figure 1). Table 1 categorizes R_4 groups by type using Fleming's frontier molecular orbital (FMO) notation of π influence,[60] where X groups are those that contain a LP-bearing atom attached to the ring, such as amino or hydroxyl, Z groups are π-withdrawing groups, such as formyl or cyano, and C groups simply extend the conjugation of the system, such as ethenyl. Table 1 also shows different orientations of the substituent for **2**, **3**, **10**, and **16**. For example, **10**, **10′**, and **10″** correspond to different orientations of the substituent R_4, where $R_4 =$ OH. **10** and **10′** have C_S symmetry with the hydroxyl H pointing toward and away from N^3, respectively. **10″** corresponds to $R_4 =$ OH, where the OH in **10** has been rotated out of plane by 90°. **10″** is not a minimum, but its lower excited-state energies, like with the rotation of the amino in **2**, support the importance of π donation into the ring at C^4. The left panel of Figure 4 shows the calculated energies for the excited states in order of increasing S_1 energies for all C^4 derivatives in this study, identified by their number label. For reference, **1** is in the middle ($R_4 = R_5 =$ H). The trend shows that C^4-X groups increase all three excited-state energies relative to 2P, while Z and C groups both lower excitation energies relative to 2P, with Z groups having a larger energy-lowering effect than C groups. The range of S_1 energies for all C^4 derivatives is about 1 eV. It should be noted here that **10** is a tautomer of uracil (U), which has a C^4 carbonyl and N^3-H. By the above arguments, U should have a particularly high absorbance energy, based on a strong C^4-O π bond. Indeed, MRCI energy (14,10 CAS) for the $\pi\pi^*$ state (S_2) of the MP2 C_S GS geometry is 6.08 eV, about 1.6 eV higher than 2P, and about 1.2 eV higher than Cyt. Also shown in Table 1 and Figure 4, as reference, are the experimentally determined

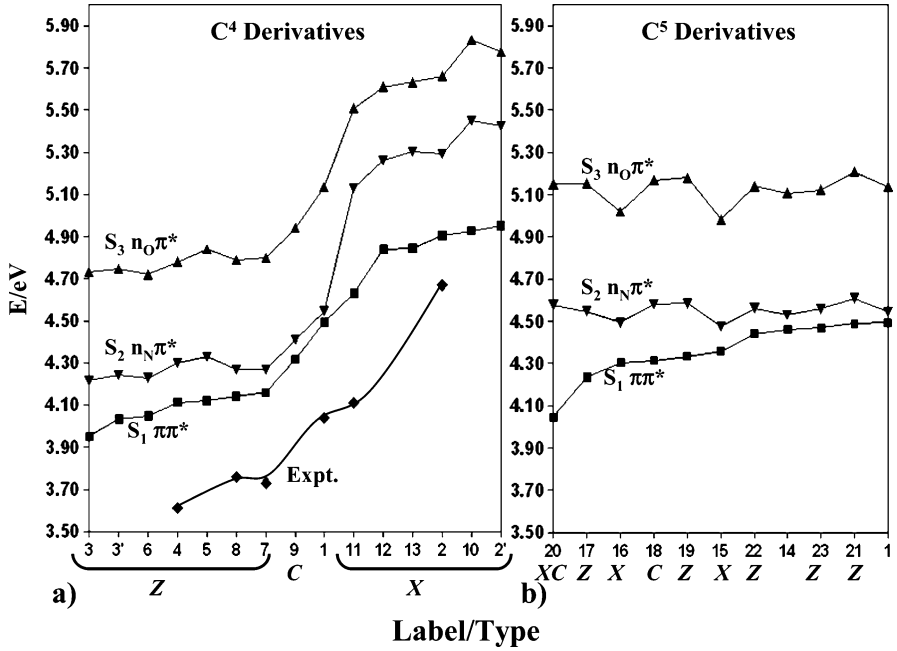

Figure 4. First three MRCI excited-state energies for (a) C^4- and (b) C^5-substituted 2P derivatives, by label number itemized in Table 1. In each panel, the order is increasing S_1 energies from left to right. In (a) the black diamonds toward the bottom correspond to experimental absorption maxima for derivatives in neutral aqueous solution, as listed in Table 1.

energies corresponding to absorption λ_{max} values for several C^4 derivatives in aqueous pH = 7 environments. While there is clearly a systematic error associated with MRCI in calculating $\pi\pi^*$ energies about 10% higher than experimental values, which has been addressed before,[16,39] the calculated energetic trend for the S_1 $\pi\pi^*$ states of C^4 derivatives follows the experimental trend well. Our results model gas phase rather than aqueous solution, although the solvent effect is not expected to be as high as the differences with the experiment observed here.

If the influence on energies is related to π interaction from R_4, then the bond length for the bond between C^4 and the first atom of R_4 should reflect it, with π donation corresponding to a shortening of this bond and π withdrawal corresponding to a lengthening of this bond. Figure 5 shows the S_1 energies for C^4 derivatives where the R_4 atom attached to the ring is N, which we define here as N′ (to be consistent between C^4-N derivatives which carry different numbering systems). For these derivatives shortening this exocyclic bond length corresponds to a higher S_1 energy, with close to linear dependence. C^4-X derivatives display the shortest C^4-N' bonds and the highest S_1 energies, while C^4-Z derivatives display the longest C^4-N' bonds and the lowest S_1 energies. ϵ-Cyt and ϵ-CytH$^+$ both display high S_1 energies and follow this trend and will be discussed further in section 3.4.

The trend in the S_1 $\pi\pi^*$ energies for the C^4 derivatives also correlates well with the Hammett subsituent parameter, σ_P^+, an empirically derived parameter used to describe the extent of electron donation and withdrawal of substituents in terms of influence on reaction rates in aromatic systems.[61−63] The linear relationship between absorption energies and Hammett constants has been known for decades for substituted aromatic dyes,[49,64−67] and recently this relationship was demonstrated for the absorption energies of substituted cumyloxyl radicals.[68] To the best of our knowledge, such a relationship has not been reported for substituted 2-pyrimidinones. Figure 6 shows a plot of S_1 MRCI energies for C^4 derivatives with respect to σ_P^+ for substituents which have available values for σ_P^+. Also shown in the plot, for comparison, are the experimental data for those derivatives which have reported absorption spectra, and the linear regression trend lines for each series. The trend line equation for the MRCI data is $y = -0.544x + 4.47$ with $R^2 = 0.935$, and for the experimental data the trend line is $y = -0.581x + 4.01$ with $R^2 = 0.995$. Although the linear correlation for the MRCI series is not excellent, the essentially parallel nature of the two trends certainly implies that MRCI can be quite predictive of absorption energies for C^4 derivatives of 2P, and that this energetic trend follows similar trends seen in the absorption energies of substituted dyes. The MRCI S_2 $n_N\pi^*$ and S_3 $n_O\pi^*$ energies for the C^4 derivatives also correlate linearly with σ_P^+, with the trend line equation $y = -0.739x + 4.77$ ($R^2 = 0.888$) for the S_2 data and $y = -0.643x + 5.23$ ($R^2 = 0.916$) for the S_3 data. To our knowledge, there is no experimental data for these dark states, and so comparisons with experiment cannot be made.

3.3. C^5 Substituents. The previous section demonstrated the effect of different types of substituents at the C^4 position on excitation energies. This raises the question of how important the C^4 position is compared to other ring positions. In this section we explore the effect of different substituents at the C^5 position. The right panel of Figure 4 shows the energies of the C^5 derivatives in the order of increasing S_1. **1** is the reference in this series, with the highest S_1 energy. Here the trend is very different from that of the C^4 derivatives. Substitutions at C^5 all give S_1 energies lower than that of **1**, and S_2 and S_3 $n\pi^*$ energies are similar to or somewhat higher than **1**. The range for S_1 energies in this series is much smaller than that of the C^4 derivatives (about 0.4 eV), although for most derivatives the S_1 energy is much closer to that of **1**. This smaller energy effect seems to be due to resonance limitations from the C^5 group with the C^5-C^6 π bond. The N^1 π electron pair impedes resonance from the C^5-C^6 π bond into the carbonyl oxygen, in contrast with a C^4-X group, which donates a pair of electrons into a resonance system that can extend through N^3 and on into the carbonyl oxygen. Thus, the $C-N^3$ bond is "softer", while the C^5-C^6 bond is "harder", translating into a smaller overall effect from some C^5 substituent. There is notably less grouping of the R_5 types in terms of S_1 energy influence, unlike the series of C^4 derivatives. To the best of our knowledge, none of the C^5

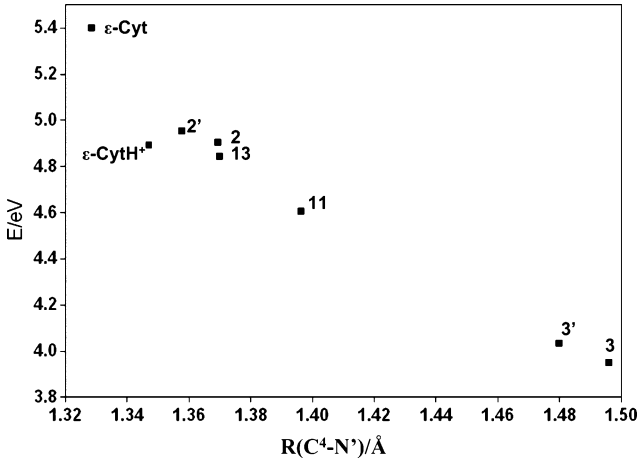

Figure 5. Plot of S_1 ($\pi\pi^*$) energies (MRCI), in eV, for C^4 derivatives containing a C^4-N' bond, as defined in the text, with respect to the C^4-N' bond length, in Å.

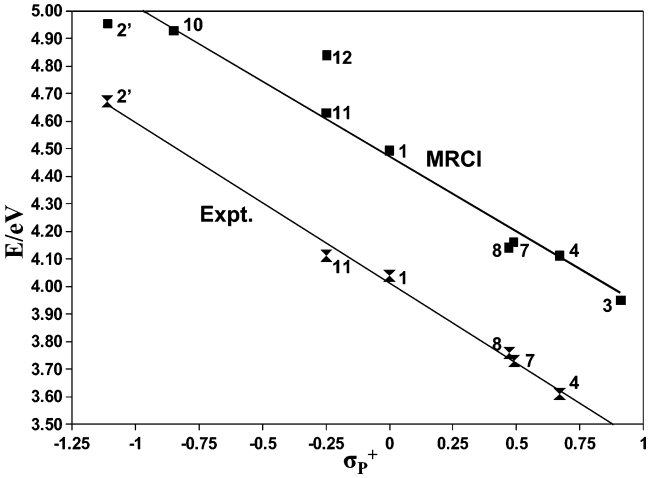

Figure 6. Plot of S_1 ($\pi\pi^*$) energies in eV with respect to the Hammett substituent parameter σ_P^+. Black squares indicate MRCI energies, and black hourglasses correspond to experimental absorption maxima for derivatives in aqueous solution, as listed in Table 1.

derivatives presented in this report have corresponding experimental absorption data reported in the literature, so validation of these results is not currently possible. A simple explanation for this type-independent S_1 energy lowering effect, using an FMO description, is presented in section 4. What is interesting here is that when an amino is at C^5 (**16**), the effect is to *lower* S_1, but when an amino is at C^4 (**2**), the effect is to *raise* S_1, both compared to 2P. Additionally, rotation of the amino by 90° either at C^4 (**2″**) or C^5 (**16″**), minimizing π donation into the ring, eliminates *both* C^4 and C^5 effects, with all excitation energies becoming close to those of 2P. This shows that both orientation and *position* of the amino group in Cyt is critical for its high excitation energy. It should be noted here that when the C^5-amino derivative is constrained to C_S symmetry (**16′**), this effect of lowering S_1 is enhanced relative to the GS geometry, where the amino is pyramidalized and rotated about 14° with respect to the ring plane.

3.4. ϵ-Cyt, ϵ-CytH$^+$, and p-Cyt. Three experimentally used cytosine analogs, ϵ-Cyt, ϵ-CytH$^+$, and p-Cyt, were included in this study to make connection with the derivatives presented in sections 3.2 and 3.3 and to check the broadness and applicability of our conclusions. The structures of these three Cyt analogs are shown in Figure 1 and their calculated and experimentally determined excited-state energies are given in Table 1. They contain similar functionality in their six-member ring compared to Cyt, and their absorption and emission properties have been studied experimentally,[69,70] as well as theoretically.[45,46] ϵ-Cyt has the highest S_1 $\pi\pi^*$ calculated energy of all the compounds presented in this study, at 5.40 eV. This energy correlates well with the C^4-N' bond length (C^4-N^9 using correct ϵ-Cyt numbering, Figure 1), which is 1.33 Å: primarily a full double bond. Figure 5 shows that this energy is in line with the trend of S_1 with respect to the C^4-N' bond for all derivatives containing this bond. Experimentally, ϵ-Cyt does not fluoresce, but the low-pH form (ϵ-CytH$^+$) does.[69] The calculated S_1 $\pi\pi^*$ energy for ϵ-CytH$^+$ is 5 eV, lower than the free-base form. Figure 5 shows that the C^4-N' bond length is 1.35 Å, which is also in line with the trend shown in the plot. Because the N^3 LP for these two forms of ϵ-Cyt is now π in character, rather than nonbonding as in the case of the C^4 derivatives of 2P, the S_2 and S_3 states are different than the C^4 derivatives. For ϵ-Cyt S_2 is $n_N\pi^*$ from excitation of the N^9 LP. S_3 is, like 2P, $n_O\pi^*$ from O^2 LP excitation. For ϵ-CytH$^+$,N^9 has lost its LP to an $N-H$ σ bond, and S_2 and S_3 are both $n_O\pi^*$ states.

Pyrrolocytosine (p-Cyt, Figure 1, Table 1) is essentially a C^4 *and* C^5 derivative. This Cyt analog is experimentally known to absorb at 3.61 eV, and it fluoresces.[70] The second ring system creates a possible C^4-X scenario from N^7, and a C^5-C or C^5-X from C^9, depending on the conjugation of the $N^7-C^8=C^9$ system. Given the very low calculated energy of S_1 of 3.95 eV, and the equally low experimental excitation energy, it seems reasonable that the C^5-C or C^5-X scenarios, both of which lower S_1, dominate the C^4-X scenario, which would raise S_1, compared to 2P. This is supported by comparing the MRCI results on p-Cyt with two derivatives: **13** and **20**. **20** is like p-Cyt with the C^4-N^7 bond cleaved, and **13** is like p-Cyt with the C^5-C^9 bond cleaved. S_1 for **20** is 4.11 eV, very close to that of p-Cyt, while S_1 for **13** is 4.98 eV, about 1 eV higher than that for p-Cyt. Since the C^4-N^7 bond length is close to that of Cyt, at 1.37 Å, but the excitation energy for p-Cyt is very low, it appears that the S_1 energy of p-Cyt is influenced more by π conjugation extension at C^5 than π donation at C^4.

What is most interesting about these experimental cytosine analogs is that fluorescence behavior seems to correlate with lower vertical excitation energy as in the case of 5M2P.

4. Frontier Molecular Orbital (FMO) Description of C^4 and C^5 Effects

This section gives a qualitative description of the S_1 effects at C^4 and C^5 for derivatives presented in sections 3.2 and 3.3 in terms of FMO theory, which describes the effects of substituents on conjugated systems primarily in terms of the highest occupied π molecular orbital (HOMO) and the lowest unoccupied π molecular orbital (LUMO).[60] In general, the effect of the addition of an electron-donating (X) group to a conjugated system is to raise the energies of both the HOMO and LUMO. An electron-withdrawing (Z) group lowers both HOMO and LUMO energies. In both cases the overall effect of the substituent on the energy of the $\pi\pi^*$ state depends on the relative magnitude of energy change of the HOMO compared to that of the LUMO. A conjugation extending group (C) raises the HOMO energy and lowers the LUMO energy, lowering the energy of the $\pi\pi^*$ state. The n orbitals are of different symmetry than π orbitals, and thus their energies are not significantly affected by additional substituents. However, since an $n\pi^*$ state involves excitation into the LUMO, which can be influenced by additional substituents, the energies of $n\pi^*$ states can also be similarly changed by substituents.

Figure 7 shows the HOMO and LUMO orbitals for the S_1 $\pi\pi^*$ state for selected C^4 and C^5 derivatives, along with their

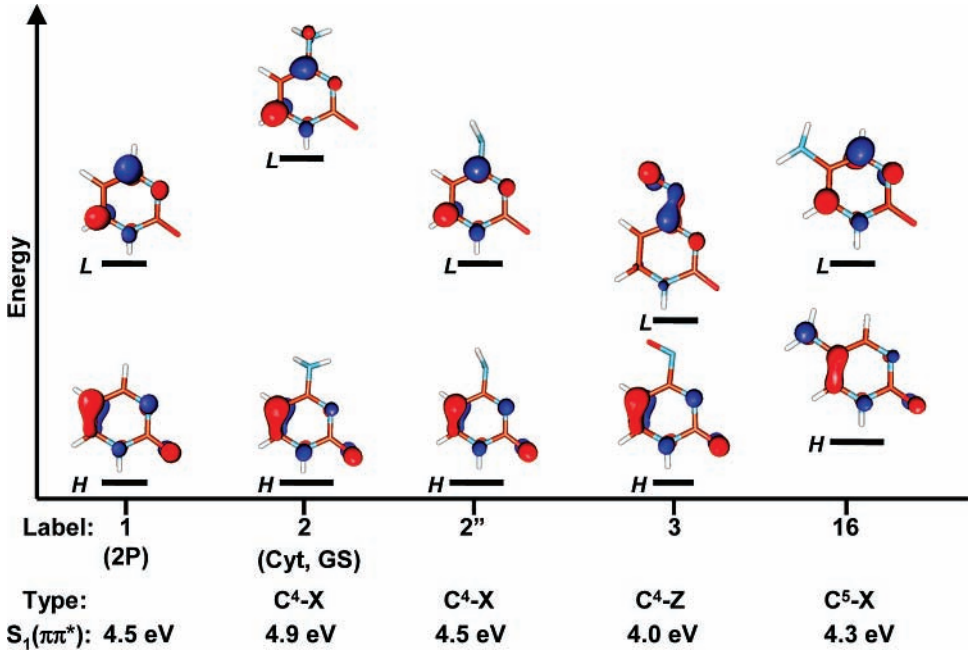

Figure 7. HOMO (H) and LUMO (L) orbitals dominating the S_1 ($\pi\pi^*$) state for selected C^4 and C^5 derivatives. Label, group type, and S_1 energy (MRCI) are listed for each derivative along the bottom. The energies shown for each HOMO−LUMO pair are qualitative and relative based on S_1 energies and general orbital character, with the reference system 2P shown to the far left.

number label, R_4 or R_5 group type, and their S_1 energies. The HOMO−LUMO gaps shown are qualitative and given for relative comparison with **1**, the reference system. The electron density in the ring system for the substituted 2P molecules is in most cases very similar to that of 2P. The HOMO for GS Cyt (**2**, $R_4 = NH_2 = \mathbf{X}$) has a node through the ring carbon atom and the nitrogen of the amino group, so the HOMO energy is not affected significantly by the substituent. The LUMO for Cyt, however, is destabilized compared to that of 2P because of the antibonding overlap between the ring carbon and nitrogen (on the C^4-N^4 bond). Rotating the amino 90° (**2″**) removes the π nature of its LP, and the LUMO for this orientation has similar density to that of 2P, and thus similar energy. This is reflected in the calculated S_1 energies of **1** and **2″**, which are close to equal. An electron-withdrawing group (Z) at C^4, such as NO in the case of **3,** creates, like **2**, no change in the HOMO, but the LUMO displays π overlap character on the C^4-N' bond, as well as withdrawal of density at N^1 and C^6, compared to 2P. These two effects act to lower the LUMO of this derivative, reflected in S_1 being about 0.5 eV lower than that of **1**. In all of the above cases the LUMO is affected by the presence of the substituent so this effect will also be present in the excitation energies of the nπ^* states S_2 and S_3. These results show that substituent effects at C^4 follow clear patterns, both in energies and in FMO description, in terms of substituent type. Such is less in the case with the C^5 derivatives.

Since the energy range for the C^5 derivatives is much smaller than that of the C^4 derivatives, the trends predicted by FMO theory may not be the dominant contributions to the excitation energies of those molecules, and FMO theory may not be adequate to describe the observed trends. All of the substituents at this position to some degree lower the S_1 energy compared to **1**. In **16**, the C^5 substituent is an electron-donating amino group. This example is a good illustration (Figure 7), and important, since this derivative is Cyt with the amino moved to C^5. The situation is similar to Cyt but the effects on the HOMO and LUMO are now switched. The energy for the HOMO is destabilized compared to that of 2P because of the antibonding overlap between C^5 and amino group. The LUMO is not affected significantly since there is a node through these atoms and thus the amino group does not change the overall electron density in the orbital much.

The above analysis implies that the substituent effect is dominant at the GS planar geometry. At the distorted geometries along the S_1 PES, however, these effects should become less important, and the S_1 energies of the different derivatives presented in this study could become comparable. This difference will have an effect on the photophysical properties, as is seen in Cyt and 5M2P (Figure 2). However, theoretical predictions of fluorescence or radiationless decay behavior for a particular derivative cannot be made based solely on effects on vertical excitation. For prediction of emission properties, a thorough and accurate theoretical analysis of the entire S_1 PES, especially regions far from the Franck−Condon region, must be made, as was discussed in section 1.

5. Conclusions

In this report we have presented a theoretical analysis of the influence on the bright vertical excitation energies of C^4- and C^5-substituted derivatives of 2-pyrimidin-(*H*1)-one (2P). Results of MRCI calculations indicate that the presence, position, and orientation of the C^4-amino group in Cyt has direct impact on the S_1 $\pi\pi^*$ energy, as well as the energy of the two dark nπ^* states. Derivatives of 2P with π-donating groups (C^4-X) display increased S_1 energies compared to 2P, dependent on the amount of π donation of the group, by destabilizing the LUMO relative to the HOMO. This effect is effectively switched off by rotating the group 90° out of the ring plane so that the π interaction is removed. 2P derivatives with π withdrawing (C^4-Z) or simple conjugation extension (C^4-C) in general display lower S_1 energies than 2P, by stabilizing the LUMO relative to the HOMO. A linear correlation between the S_1 energies and the Hammett substituent parameter σ_P^+ is demonstrated for C^4-X and C^4-Z derivatives, both for the calculated MRCI energies and data from the experimentally determined absorption spectra. 2P derivatives with substitution at C^5 tend to display a much smaller effect, with S_1 energies lower than 2P, regardless of

the type of substituent. In addition, the high vertical excitations of ϵ-Cyt and ϵ-CytH$^+$ are attributed to strong π donation at C^4, creating a full C^4−N^9 double bond, whereas the low vertical excitation of p-Cyt is attributed to π conjugation extension at C^5. Comparisons with experimental data of known 2P derivatives show that these trends are quite predictive for excitation energies and could be used for other similar 2P derivatives, such as artificial DNA pyrimidines, where particular absorbance properties are desired. In particular, the linear correlation between excited-state energies and σ_P^+ for the C^4 derivatives could be used for quantitative prediction of absorption maxima. The differences in vertical excitation energies could also have an effect on the overall photophysical (fluorescence) properties of the derivatives.

Acknowledgment. This work was supported by the National Science Foundation under Grant No. CHE-0449853 and Temple University.

Supporting Information Available: Cartesian coordinates for all compounds presented in this report are available. This material is available free of charge via the Internet at http://pubs.acs.org.

References and Notes

(1) Crespo-Hernandez, C. E.; Cohen, B.; Hare, P. M.; Kohler, B. *Chem. Rev.* **2004**, *104*, 1977.
(2) Ullrich, S.; Schultz, T.; Zgierski, M. Z.; Stolow, A. *Phys. Chem. Chem. Phys.* **2004**, *6*, 2796.
(3) Kang, H.; Lee, K. T.; Jung, B.; Ko, Y. J.; Kim, S. K. *J. Am. Chem. Soc.* **2002**, *124*, 12958.
(4) Canuel, C.; Mons, M.; Piuzzi, F.; B. Tardivel; Dimicoli, I.; Elhanine, M. *J. Chem. Phys.* **2005**, *122*, 074316.
(5) Ismail, N.; Blancafort, L.; Olivucci, M.; Kohler, B.; Robb, M. *J. Am. Chem. Soc.* **2002**, *124*, 6818.
(6) Merchán, M.; Serrano-Andrés, L. *J. Am. Chem. Soc.* **2003**, *125*, 8108.
(7) Blancafort, L.; Robb, M. A. *J. Phys. Chem. A* **2004**, *108*, 10609.
(8) Sobolewski, A. L.; Domcke, W. *Phys. Chem. Chem. Phys.* **2004**, *6*, 2763.
(9) Tomić, K.; Jörg, T.; Marian, C. M. *J. Phys. Chem. A* **2005**, *109*, 8410.
(10) Zgierski, M. Z.; Patchkovskii, S.; Lim, E. C. *J. Chem. Phys.* **2005**, *123*, 081101.
(11) Merchán, M.; Serrano-Andrés, L.; Robb, M.; Blancafort, L. *J. Am. Chem. Soc.* **2005**, *127*, 1820.
(12) Kistler, K. A.; Matsika, S. *J. Phys. Chem. A* **2007**, *111*, 2650.
(13) *Conical Intersections: Electronic Structure, Dynamics & Spectroscopy*; Domcke, W., Yarkony, D. R., Köppel, H., Eds.; World Scientific Publishing Co. Pte. Ltd.: Singapore, 2004; Vol. 15.
(14) Yarkony, D. R. *J. Phys. Chem. A* **2001**, *105*, 6277.
(15) Matsika, S. Conical Intersections in Molecular Systems. In *Reviews in Computational Chemistry*; Lipkowitz, K. B., Cundari, T. R., Eds.; John Wiley & Sons, Inc.: Hoboken, NJ, 2007; Vol. 23, pp 83.
(16) Kistler, K. A.; Matsika, S. *Photochem. Photobiol.* **2007**, *83*, 611.
(17) Žaloudek, F.; Novros, J. S.; Clark, L. B. *J. Am. Chem. Soc.* **1985**, *107*, 7344.
(18) Nir, E.; Miller, M.; Grace, L. I.; deVries, M. S. *Chem. Phys. Lett.* **2002**, *355*, 59.
(19) Laland, S. G.; Serck-Hanssen, G. *Biochem. J.* **1964**, *90*, 76.
(20) Rappaport, H. P. *Nucl. Acids Res.* **1988**, *16*, 7253.
(21) Wu, P.; Norland, T. M.; Gildea, B.; McLaughlin, L. W. *Biochem.* **1990**, *29*, 6508.
(22) Malone, R. J.; Miller, A. M.; Kohler, B. *Photochem. Photobiol.* **2003**, *77*, 158.
(23) Smagowicz, J.; Wierzchowski, K. L. *Acta. Phys. Polon.* **1968**, *34*, 365.
(24) Häupl, T.; Windolph, C.; Jochum, T.; Brede, O.; Hermann, R. *Chem. Phys. Lett.* **1997**, *280*, 520.
(25) Nir, E.; Kleinermanns, K.; Grace, L.; Vries, M. S. d. *J. Phys. Chem. A* **2001**, *105*, 5106.
(26) Seefeld, K. A.; Plützer, C.; Löwenich, D.; Häber, T.; Linder, R.; Kleinermanns, K.; Tatchen, J.; Marian, C. M. *Phys. Chem. Chem. Phys.* **2005**, *7*, 3021.
(27) Mennucci, B.; Toniolo, A.; Tomasi, J. *J. Phys. Chem. A* **2001**, *105*, 4749.
(28) Matsika, S. *J. Phys. Chem. A* **2005**, *109*, 7538.
(29) Perun, S.; Sobolewski, A. L.; Domcke, W. *Chem. Phys.* **2005**, *313*, 107.
(30) Perun, S.; Sobolewski, A. L.; Domcke, W. *J. Am. Chem. Soc.* **2005**, *127*, 6257.
(31) Serrano-Andres, L.; Merchan, M.; Borin, A. C. *Proc. Natl. Acad. Sci. U.S.A.* **2006**, *103*, 8691.
(32) Rachofsky, E. L.; Ross, J. B. A.; Krauss, M.; Osman, R. *J. Phys. Chem. A* **2001**, *105*, 190.
(33) Jean, J. M.; Hall, K. B. *Biochemistry* **2002**, *41*, 13152.
(34) Broo, A.; Holmén, A. *J. Phys. Chem. A* **1997**, *101*, 3589.
(35) Fülscher, M. P.; Roos, B. O. *J. Am. Chem. Soc.* **1995**, *117*, 2089.
(36) Zgierski, M. Z.; Patchkovskii, S.; Fujiwara, T.; Lim, E. C. *J. Phys. Chem. A* **2005**, *109*, 9384.
(37) Petke, J. D.; Maggiora, G. M.; Christoffersen, R. E. *J. Phys. Chem.* **1992**, *96*, 6992.
(38) Sobolewski, A. L.; Domcke, W. *Eur. Phys. J. D* **2002**, *20*, 369.
(39) Matsika, S. *J. Phys. Chem. A* **2004**, *108*, 7584.
(40) Nguyen, M. T.; Zhang, R.; Nam, P.-C.; Ceulemans, A. *J. Phys. Chem. A* **2004**, *108*, 6554.
(41) Nielsen, S. B.; Sølling, T. I. *Chem. Phys. Chem.* **2005**, *6*, 1276.
(42) Perun, S.; Sobolewski, A. L.; Domcke, W. *J. Phys. Chem. A* **2006**, *110*, 13238.
(43) Blancafort, L. *J. Am. Chem. Soc.* **2006**, *128*, 210.
(44) Lorentzon, J.; Fülscher, M. P.; Roos, B. O. *J. Am. Chem. Soc.* **1995**, *117*, 9265.
(45) Major, D. T.; Fisher, B. *J. Phys. Chem. A* **2003**, *107*, 8923.
(46) Thompson, K. C.; Miyake, N. *J. Phys. Chem. B* **2005**, *109*, 6012.
(47) Lewis, G. N. *J. Am. Chem. Soc.* **1945**, *67*, 770.
(48) Vittum, P. W.; Brown, G. H. *J. Am. Chem. Soc.* **1947**, *69*, 152.
(49) Brown, G. H.; Figueras, J.; Gledhill, R. J.; Kibler, C. J.; McCrossen, F. C.; Parmerter, S. M.; Vittum, P. W.; Weissberger, A. *J. Am. Chem. Soc.* **1957**, *79*, 2919.
(50) Ichijima, S.; Kobayashi, H. *Bull. Chem. Soc. Jpn.* **2005**, *78*, 1929.
(51) Yang, G. B.; Wu, Y.; Tian, W. J.; Zhou, X.; Ren, A. M. *Curr. Appl. Phys.* **2005**, *5*, 327.
(52) Davi, W. B.; Ki, M. R. W. I.; Ratner, M. A. *Int. J. Quantum Chem.* **1999**, *72*, 463.
(53) Frisch, M. J.; Trucks, G. W.; Schlegel, H. B.; Scuseria, G. E.; Robb, M. A.; Cheeseman, J. R.; Montgomery, J. A., Jr.; Vreven, T.; Kudin, K. N.; Burant, J. C.; Millam, J. M.; Iyengar, S. S.; Tomasi, J.; Barone, V.; Mennucci, B.; Cossi, M.; Scalmani, G.; Rega, N.; Petersson, G. A.; Nakatsuji, H.; Hada, M.; Ehara, M.; Toyota, K.; Fukuda, R.; Hasegawa, J.; Ishida, M.; Nakajima, T.; Honda, Y.; Kitao, O.; Nakai, H.; Klene, M.; Li, X.; Knox, J. E.; Hratchian, H. P.; Cross, J. B.; Adamo, C.; Jaramillo, J.; Gomperts, R.; Stratmann, R. E.; Yazyev, O.; Austin, A. J.; Cammi, R.; Pomelli, C.; Ochterski, J. W.; Ayala, P. Y.; Morokuma, K.; Voth, G. A.; Salvador, P.; Dannenberg, J. J.; Zakrzewski, V. G.; Dapprich, S.; Daniels, A. D.; Strain, M. C.; Farkas, O.; Malick, D. K.; Rabuck, A. D.; Raghavachari, K.; Foresman, J. B.; Ortiz, J. V.; Cui, Q.; Baboul, A. G.; Clifford, S.; Cioslowski, J.; Stefanov, B. B.; Liu, G.; Liashenko, A.; Piskorz, P.; Komaromi, I.; Martin, R. L.; Fox, D. J.; Keith, T.; Al-Laham, M. A.; Peng, C. Y.; Nanayakkara, A.; Challacombe, M.; Gill, P. M. W.; Johnson, B.; Chen, W.; Wong, M. W.; Gonzalez, C.; Pople, J. A. *Gaussian 03*, revision A.1; Gaussian, Inc.: Pittsburgh, PA, 2003.
(54) Dunning, T. H. *J. Chem. Phys.* **1989**, *90*, 1007.
(55) Lischka, H.; Shepard, R.; Shavitt, I.; Pitzer, R. M.; Dallos, M.; Müller, T.; Szalay, P. G.; Brown, F. B.; Ahlrichs, R.; Böhm, H. J.; Chang, A.; Comeau, D. C.; Gdanitz, R.; Dachsel, H.; Ehrhardt, C.; Ernzerhof, M.; Höchtl, P.; Irle, S.; Kedziora, G.; Kovar, T.; Parasuk, V.; Pepper, M. J. M.; Scharf, P.; Schiffer, H.; Schindler, M.; Schüler, M.; Seth, M.; Stahlberg, E. A.; Zhao, J.-G.; Yabushita, S.; Zhang, Z. COLUMBUS, an *Ab Initio* Electronic Structure Program, Release 5.8, 2001.
(56) Lischka, H.; Shepard, R.; Pitzer, R. M.; Shavitt, I.; Dallos, M.; Müller, T.; Szalay, P. G.; Seth, M.; Kedziora, G. S.; Yabushita, S.; Zhang, Z. *Phys. Chem. Chem. Phys.* **2001**, *3*, 664.
(57) Lischka, H.; Shepard, R.; Brown, F. B.; Shavitt, I. *Int. J. Quantum Chem.: Quantum Chem. Symp.* **1981**, *15*, 91.
(58) Schaftenaar, G.; Noordik, J. H. *J. Comput.-Aided Mol. Des.* **2000**, *14*, 123.
(59) *Handbook of Chemistry and Physics*, 65th ed.; Weast, R. C., Ed.; CRC Press, Inc.: Boca Raton, FL, 1984−1985.
(60) Fleming, I. *Frontier Orbitals and Organic Chemical Reactions*; John WIley & Sons, Ltd.: New York, 1976.
(61) Hammett, L. P. *Chem. Rev.* **1935**, *17*, 125.
(62) Gordon, A. J.; Ford, R. A. *The Chemist's Companion. A Handbook of Practical Data, Techniques, and References*; John Wiley & Sons: New York, 1972.
(63) Krygowski, T. M.; Stępień, B. T. *Chem. Rev.* **2005**, *105*, 3482.
(64) Ross, D. L.; Reissner, E. *J. Org. Chem.* **1966**, *31*, 2571.
(65) Irick, G. J.; Pacifici, J. G. *Text. Res. J.* **1972**, *42*, 391.
(66) Togashi, D. M.; Nicodem, D. E. *Spectrochim. Acta., Part A* **2004**, *60*, 3205.

(67) Chao, C.-C.; Leung, M.; Su, Y. O.; Chiu, K.-Y.; Lin, T.-H. *J. Org. Chem.* **2005**, *70*, 4323.

(68) Baciocchi, E.; Bietti, M.; Salamone, M.; Steenken, S. *J. Org. Chem.* **2002**, *67*, 2266.

(69) Barrio, J. R.; Sattsangi, P. D.; Gruber, G. A.; Dammann, L. G.; Leonard, N. J. *J. Am. Chem. Soc.* **1976**, *98*, 7408.

(70) Berry, D. A.; Jung, K.-Y.; Wise, D. S.; Sercel, A. D.; Pearson, W. H.; Mackie, H.; Randolph, J. B.; Somers, R. L. *Tetrahedron Lett.* **2004**, *45*, 2457.

(71) Beak, P.; Fry, F. S. J.; Lee, J.; Steele, F. *J. Am. Chem. Soc.* **1975**, *98*, 171.

(72) Sharonov, A.; Gustavsson, T.; Carré, V.; Renault, E.; Markovitski, D. *Chem. Phys. Lett.* **2003**, *380*, 173.

(73) Klein, R. S.; Wempen, I.; Watanabe, K. A.; Fox, J. J. *J. Org. Chem.* **1970**, *35*, 2330.

(74) Völkel, W.; Dekant, W. *Chem. Res. Toxicol.* **1998**, *11*, 1082.